J Therm Anal Calorim (2011) 103:373–380
DOI 10.1007/s10973-010-0880-z

Exceptional thermal stability and thermodynamic properties of lithium based metal–organic framework

Chun-Hong Jiang · Li-Fang Song · Cheng-Li Jiao · Jian Zhang · Li-Xian Sun · Fen Xu · Yong Du · Zhong Cao

Received: 24 February 2010 / Accepted: 6 May 2010 / Published online: 29 May 2010

Abstract A three-dimensional lithium-based metal–organic framework Li_2(2,6-NDC) (2,6-NDC = 2,6-naphthalene dicarboxylate) has been synthesized solvothermally and characterized by X-ray powder diffraction, elemental analysis, FT-IR spectroscopy, thermogravimetry and mass spectrometer analysis (TG–MS). The framework has exceptional stability and is stable to 863 K. The thermal decomposition characteristic of this compound was investigated through the TG–MS from 293 to 1250 K. The molar heat capacity of the compound was measured by temperature modulated differential scanning calorimetry (TMDSC) over the temperature range from 195 to 670 K for the first time. The thermodynamic parameters such as entropy and enthalpy versus 298.15 K based on the above molar heat capacity were calculated.

C.-H. Jiang · L.-F. Song · C.-L. Jiao · J. Zhang · L.-X. Sun (✉)
Materials and Thermochemistry Laboratory, Dalian Institute of Chemical Physics, Chinese Academy of Sciences, 457 Zhongshan Road, Dalian 116023, People's Republic of China
e-mail: lxsun@dicp.ac.cn

F. Xu (✉)
Faculty of Chemistry and Chemical Engineering, Liaoning Normal University, Dalian 116029, People's Republic of China
e-mail: xufen@lnnu.edu.cn

C.-H. Jiang · L.-F. Song · C.-L. Jiao
Graduate School of the Chinese Academy of Sciences, Beijing 100049, People's Republic of China

Y. Du
State Key Laboratory of Powder Metallurgy, Central South University, Changsha 410083, People's Republic of China

Z. Cao
School of Chemistry and Environmental Engineering, Changsha University of Science and Technology, Changsha 410076, People's Republic of China

Keywords Lithium · Molar heat capacity · Metal–organic frameworks · TG · TMDSC

Introduction

The past decade has evidenced a growing interest in the synthesis and structural characterization of new porous crystalline architectures built from the combination of inorganic building unites with rigid organic polycarboxylates as linkers. This new emerging class of hybrid materials called metal–organic frameworks (MOF) may potentially find many applications in the field of gas storage [1–6], separation [7–10], catalysis [11, 12], and luminescence [13–16]. Because of their structural rigidity and the flexibility of the mode of coordination for the carboxylate moiety, aromatic dicarboxylates (especially 2,6-naphthalene dicarboxylate, 2,6-NDC) are the most commonly used multifunctional ligands. Among the numerous MOF materials, most of them are constructed with transitional metals or rare earth metals, while MOFs constructed with alkali metals or alkaline-earth metals have been rarely investigated [17–20]. Furthermore, frameworks built with these light metals may exhibit higher weight capacities than those with heavy metals on gas storage, essentially due to their low volumetric density.

Till now, no report about heat capacity and thermodynamic properties of the alkali metal-based MOFs is found in the literature. Molar heat capacities of the materials at different temperatures are basic data in chemistry and engineering, from which many other thermodynamic properties such as enthalpy and entropy can be calculated. These parameters are important for both theoretical and practical purposes. Heat capacities determinations of various compounds have attracted many researchers' attention [21–26].

Temperature modulated differential scanning calorimetry (TMDSC) is one of easier and more accurate methods for determining heat capacity, and this method has been greatly developed for directly determining heat capacities for various materials isothermally and non-isothermally [27–31].

In the present work, we reported a three-dimensional lithium-based metal–organic framework Li_2(2,6-NDC) (2,6-NDC = 2,6-naphthalene dicarboxylate). The thermal decomposition characteristics of this compound were investigated by TG–MS techniques at the temperature range from 293 to 1250 K. The molar heat capacity of the compound was measured by TMDSC from 195 to 670 K, and the thermodynamic parameters such as entropy and enthalpy were also calculated.

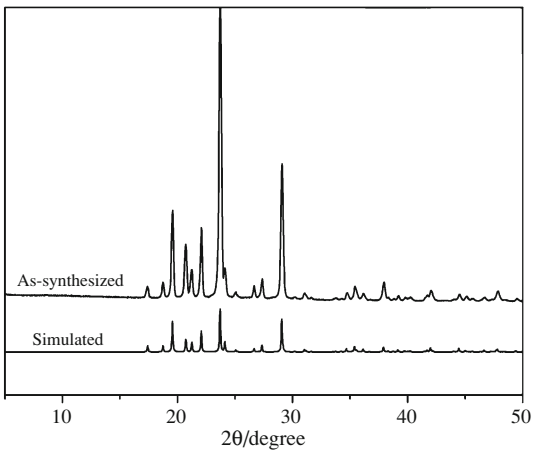

Fig. 1 PXRD patterns of As-synthesized (*top*) and Simulated patterns (*bottom*) of Li_2(2,6-NDC)

Experimental

All materials were commercially available and were of analytical grade unless stated elsewhere.

Sample preparation

Li_2(2,6-NDC) was prepared by solvothermal reaction. $LiCl{\cdot}H_2O$ (0.181 g, 3 mmol) and 2,6-NDC (0.216 g, 1 mmol) were dissolved in 24 mL *N*,*N*-dimethylformamide/tetrahydrofuran mixture (3:1 by volume). Then, the mixture was sealed in a 50-mL Teflon-lined stainless steel autoclave and heated at 150 °C for 3 days, then cooled naturally to room temperature. The resulting colorless crystals were isolated by filtration and washed thoroughly with DMF, and finally dried in vacuum at 60 °C overnight. Yield: 57.37%, based on Li.

Characterization

Elemental analysis was carried on PE-2400 II Series CHNS/O analyzer. FT-IR spectroscopy was recorded on a Nicolet 380 FT-IR spectrometer using KBr pellet in the wavelength range of 4000–400 cm^{-1}. Powder X-ray diffraction measurement was recorded on a X'Pert PRO X-ray diffractometer using Cu K_α radiation (40 kV, 40 mA). The PXRD patterns of as-synthesized (red) and simulated patterns (black) of Li_2(2,6-NDC) are shown in Fig. 1.

Elemental analysis (%) calculated for this compound: C 63.20, H 2.65; found: C 62.86, H 2.83.

FT-IR: 3050–3650 cm^{-1}, ν(O–H); 2920 cm^{-1}, ν_{as}(C–H); 2850 cm^{-1}, ν_s(C–H); 1360–1610 cm^{-1}, ν(aromatic C=C); 777–806 cm^{-1}, ν_s(aromatic C–H).

Thermal analysis

Thermogravimetric analysis (TG) was carried out on Cahn Thermax 500 from 293 to 1250 K. The heating rate was 10 K min^{-1}, and the flow rate of air was 100 mL min^{-1}. The mass of the compound was about 46.20 mg. The TG equipment was calibrated by the $CaC_2O_4{\cdot}H_2O$ (99.9%). Mass spectra (MS) were performed on a Multicomponent Online Gas Analyzer GAM 200.

Heat capacity measurement

Heat capacity measurements were performed on DSC Q1000 (T-zero DSC-technology, TA Instruments Inc., USA) with a heating rate of 10 K min^{-1}. Dry high purity nitrogen (99.999%) was used as purge gas at a flow rate of 50 mL min^{-1} through the DSC cell. And a mechanical cooling system was used for the experimental measurement. The temperature scale of the instrument was initially calibrated in the standard DSC mode, using the extrapolated onset temperatures of the melting of indium (429.75 K) as described in our previous papers [29–31]. The energy scale was calibrated with the heat of fusion of indium (28.45 J g^{-1}). The heat capacity calibration was made by running a standard sapphire (Al_2O_3) at the experimental temperature. The accuracy of TMDSC is established by comparing the measured heat capacity of standard sapphire with previously reported values [32]. The calibration method and the experiment were performed at the same conditions as follows: (1) sampling interval: 1.00 s/pt; (2) zero heat flow at 428.15 K; (3) equilibrate at 183.15 K; (4) isothermal for 5.00 min; (5) temperature ramp at 10 K min^{-1} to 673.15 K.

The masses of the reference and sample pans with lids were measured to be within 54.25 ± 0.05 mg. Samples were crimped in non-hermetic aluminum pans with lids. Sample mass was weighed on a METTLER TOLEDO electrobalance (AB135-S, Classic) with an accuracy of (±0.01 mg).

Results and discussion

TG–MS results

The TG–MS curves (Fig. 2) of Li_2(2,6-NDC) show that the framework of this compound maintains extremely high thermal stability under air atmosphere. There is no any mass loss until 863 K. From 863 to 1223 K, the mass loss refers to the framework decomposition (2,6-NDC oxidative degradation), with Li_2O as the final residue (total mass loss recorded: 85.65%; calculated: 86.90%). The MS curve shows that the gas degradation products are mainly H_2O (m/z = 18) and CO_2 (m/z = 44). Therefore, Li_2(2,6-NDC) exhibits a better thermo stability than most reported coordination polymers. This framework's high thermal stability may attributes to the lack of solvent molecules in the structure.

Heat capacity

Three reduplicate experiments (test 1, test 2, and test 3), the average, and the standard deviation of Li_2(2,6-NDC) are given in Table 1. The experimental standard deviations are below 0.021 J K^{-1} g^{-1}, and this shows reasonably good reproducibility in the experimental temperature range from 195 to 670 K. The experimental molar heat capacities curve of Li_2(2,6-NDC) versus temperature is shown in

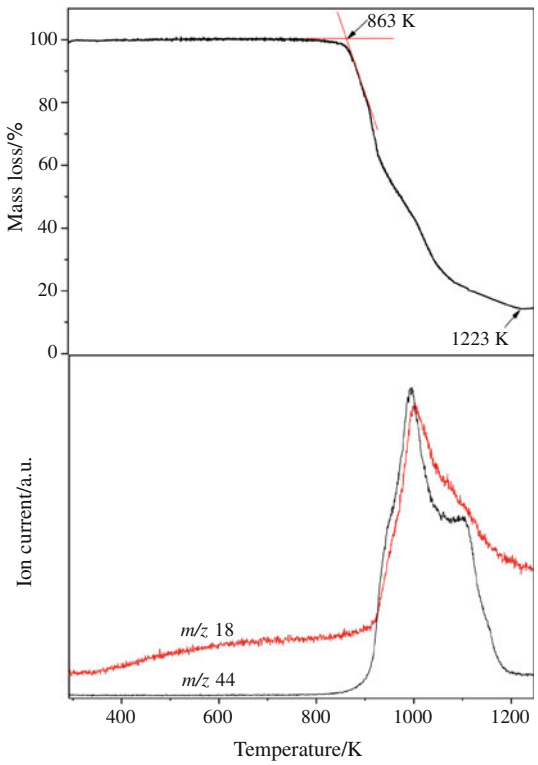

Fig. 2 TG–MS curves of Li_2(2,6-NDC) under air atmosphere at 10 K min^{-1}

Table 1 The data of three reduplicate experiments for Li_2(2,6-NDC)

T/K	$C_{p,m}$ (exp)/J K^{-1} g^{-1}				Standard deviation/ J K^{-1} g^{-1}
	Test 1	Test 2	Test 3	Average	
195	0.7653	0.7672	0.7621	0.7649	0.0026
200	0.7980	0.7994	0.7993	0.7989	0.00078
205	0.8223	0.8236	0.8275	0.8244	0.0027
210	0.8385	0.8398	0.8453	0.8412	0.0036
215	0.8551	0.8559	0.8635	0.8582	0.0046
220	0.8729	0.8737	0.8815	0.8760	0.0048
225	0.8902	0.8915	0.9004	0.8940	0.0056
230	0.9075	0.9084	0.9178	0.9112	0.0057
235	0.9234	0.9243	0.9337	0.9271	0.0057
240	0.9379	0.9399	0.9502	0.9427	0.0066
245	0.9536	0.9545	0.9662	0.9581	0.0070
250	0.9699	0.9699	0.9825	0.9741	0.0073
255	0.9887	0.9868	1.000	0.9918	0.0071
260	1.003	1.004	1.017	1.008	0.0078
265	1.020	1.020	1.034	1.025	0.0081
270	1.037	1.036	1.051	1.041	0.0084
275	1.055	1.054	1.069	1.059	0.0084
280	1.074	1.073	1.087	1.078	0.0078
285	1.093	1.092	1.107	1.097	0.0084
290	1.110	1.110	1.126	1.115	0.0092
295	1.128	1.126	1.143	1.132	0.0093
300	1.144	1.142	1.159	1.148	0.0093
305	1.161	1.159	1.175	1.165	0.0087
310	1.177	1.175	1.193	1.182	0.0099
315	1.193	1.191	1.208	1.197	0.0093
320	1.209	1.206	1.224	1.213	0.0096
325	1.225	1.222	1.239	1.229	0.0091
330	1.239	1.236	1.255	1.243	0.010
335	1.252	1.251	1.271	1.258	0.011
340	1.267	1.267	1.286	1.273	0.011
345	1.281	1.280	1.300	1.287	0.011
350	1.296	1.294	1.315	1.302	0.012
355	1.309	1.308	1.329	1.315	0.012
360	1.324	1.321	1.344	1.330	0.013
365	1.337	1.337	1.358	1.344	0.012
370	1.350	1.350	1.372	1.357	0.013
375	1.366	1.364	1.386	1.372	0.011
380	1.380	1.378	1.401	1.386	0.013
385	1.393	1.391	1.415	1.400	0.013
390	1.407	1.406	1.431	1.415	0.014
395	1.421	1.420	1.444	1.428	0.014
400	1.433	1.432	1.456	1.440	0.014
405	1.444	1.444	1.469	1.452	0.014
410	1.458	1.456	1.482	1.465	0.014
415	1.472	1.469	1.496	1.479	0.015
420	1.485	1.484	1.510	1.493	0.015
425	1.500	1.497	1.522	1.506	0.014

Table 1 continued

T/K	$C_{p,m}$ (exp)/J K^{-1} g^{-1}				Standard deviation/ J K^{-1} g^{-1}
	Test 1	Test 2	Test 3	Average	
430	1.512	1.509	1.535	1.519	0.014
435	1.523	1.521	1.549	1.531	0.016
440	1.535	1.534	1.562	1.544	0.016
445	1.549	1.547	1.573	1.556	0.014
450	1.561	1.558	1.585	1.568	0.015
455	1.572	1.57	1.598	1.580	0.016
460	1.584	1.581	1.611	1.592	0.017
465	1.596	1.593	1.622	1.604	0.016
470	1.608	1.604	1.634	1.615	0.016
475	1.620	1.616	1.647	1.628	0.017
480	1.632	1.628	1.660	1.640	0.017
485	1.643	1.640	1.671	1.651	0.017
490	1.653	1.650	1.680	1.661	0.017
495	1.663	1.662	1.691	1.672	0.016
500	1.675	1.671	1.703	1.683	0.017
505	1.684	1.682	1.714	1.693	0.018
510	1.697	1.694	1.724	1.705	0.017
515	1.708	1.706	1.734	1.716	0.016
520	1.720	1.716	1.743	1.726	0.015
525	1.730	1.726	1.754	1.737	0.015
530	1.739	1.736	1.764	1.746	0.015
535	1.750	1.746	1.773	1.756	0.015
540	1.758	1.754	1.781	1.764	0.015
545	1.768	1.765	1.790	1.774	0.014
550	1.778	1.775	1.802	1.785	0.015
555	1.787	1.783	1.812	1.794	0.016
560	1.796	1.793	1.818	1.802	0.014
565	1.804	1.802	1.827	1.811	0.014
570	1.813	1.810	1.839	1.821	0.016
575	1.823	1.818	1.848	1.830	0.016
580	1.831	1.827	1.856	1.838	0.016
585	1.838	1.835	1.865	1.846	0.017
590	1.849	1.844	1.876	1.856	0.017
595	1.856	1.850	1.884	1.863	0.018
600	1.862	1.858	1.892	1.871	0.019
605	1.872	1.867	1.905	1.881	0.021
610	1.883	1.879	1.914	1.892	0.019
615	1.893	1.888	1.923	1.901	0.019
620	1.902	1.896	1.930	1.909	0.018
625	1.910	1.903	1.936	1.916	0.017
630	1.921	1.915	1.944	1.927	0.015
635	1.931	1.926	1.951	1.936	0.013
640	1.940	1.935	1.954	1.943	0.0098
645	1.947	1.945	1.959	1.950	0.0076
650	1.958	1.956	1.969	1.961	0.0070
655	1.966	1.966	1.976	1.970	0.0058
660	1.975	1.974	1.983	1.977	0.0049
665	1.982	1.983	1.993	1.986	0.0061
670	1.990	1.989	2.001	1.993	0.0067

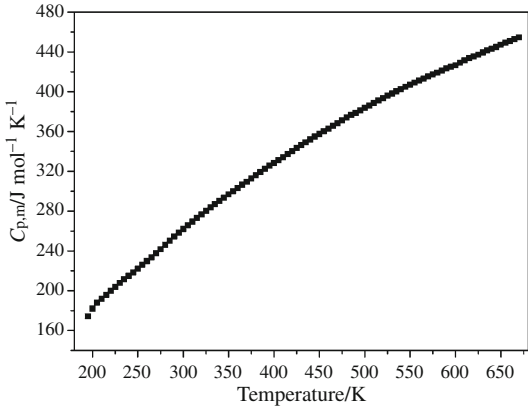

Fig. 3 Molar heat capacities ($C_{p,m}$) of Li_2(2,6-NDC) as a function of temperature

Fig. 3. The heat capacity of the sample increases continuously with the increasing temperature from 195 to 670 K. No phase transition or thermal anomaly was observed in the experimental temperature range. This indicates that Li_2(2,6-NDC) is stable in this temperature region.

The experimental and calculated molar heat capacities data are listed in Table 2. The molar heat capacities of Li_2(2,6-NDC) are fitted to the following polynomial equation of heat capacities ($C_{p,m}$) with reduced temperature (X) by means of the least square fitting.

From $T = (195 \text{ to } 670)$ K

$$C_{p,m}\ [\text{J mol}^{-1}\ \text{K}^{-1}] = 348.0 + 135.0X - 35.61X^2 + 3.246X^3 + 3.824X^4, \quad (1)$$

where $X = (T - 432.5)/237.5$ and T is the experimental temperature, 432.5 is obtained from polynomial $(T_{max} + T_{min})/2$, 237.5 is obtained from polynomial $(T_{max} - T_{min})/2$; where T_{max} is the upper limit (670 K) of the above temperature region and T_{min} is the lower limit (195 K) of the above temperature region. The correlation coefficient of the fitting, $R^2 = 0.99994$. The relative deviations of all the experimental points from the fitting heat-capacity values are within ±1.99% in Table 2. Relative deviations have been calculated by the following equation:

$$\text{RD}(\%) = 100\left[C_{p,m}(\text{exp}) - C_{p,m}(\text{fit})\right]/C_{p,m}(\text{fit}), \quad (2)$$

Table 2 The experimental and calculated molar heat capacities of Li_2(2,6-NDC)

T/K	$C_{p,m}$(exp)/J K^{-1} mol^{-1}	$C_{p,m}$(fit)/J K^{-1} mol^{-1}	RD (%)
195	174.4	178.0	−1.99
200	182.2	182.2	−0.00069
205	188.0	186.4	0.88
210	191.8	190.5	0.67
215	195.7	194.7	0.51
220	199.8	198.8	0.47
225	203.9	203.0	0.46
230	207.8	207.0	0.38
235	211.4	211.1	0.17
240	215.0	215.1	−0.066
245	218.5	219.1	−0.29
250	222.1	223.1	−0.43
255	226.2	227.1	−0.39
260	229.9	231.0	−0.48
265	233.7	234.9	−0.52
270	237.5	238.8	−0.54
275	241.6	242.6	−0.43
280	245.8	246.4	−0.24
285	250.2	250.2	0.0087
290	254.3	254.0	0.14
295	258.2	257.7	0.20
300	261.8	261.4	0.18
305	265.7	265.1	0.22
310	269.5	268.7	0.28
315	273.0	272.3	0.26
320	276.6	275.9	0.25
325	280.2	279.5	0.26
330	283.5	283.0	0.20
335	286.9	286.5	0.14
340	290.4	289.9	0.16
345	293.5	293.3	0.051
350	296.8	296.7	0.035
355	299.9	300.1	−0.046
360	303.2	303.4	−0.064
365	306.5	306.7	−0.072
370	309.5	301.0	−0.14
375	312.9	313.2	−0.10
380	316.1	316.4	−0.080
385	319.2	319.6	−0.12
390	322.6	322.7	−0.027
395	325.7	325.8	−0.021
400	328.5	328.9	−0.12
405	331.2	331.9	−0.21
410	334.2	334.9	−0.22
415	337.3	337.9	−0.17
420	340.5	340.8	−0.097
425	343.5	343.7	−0.057
430	346.3	346.6	−0.075
435	349.1	349.4	−0.082
440	352.0	352.2	−0.060
445	354.9	355.0	−0.028
450	357.6	357.8	−0.053
455	360.3	360.5	−0.047
460	363.0	363.2	−0.033
465	365.7	365.8	−0.032
470	368.4	368.4	−0.022
475	371.2	371.0	0.036
480	374.0	373.6	0.10
485	376.6	376.1	0.11
490	378.8	378.7	0.031
495	381.3	381.1	0.038
500	383.8	383.6	0.052
505	386.1	386.0	0.034
510	388.8	388.4	0.10
515	391.3	390.8	0.13
520	393.7	393.1	0.14
525	396.0	395.5	0.14
530	398.2	397.8	0.12
535	400.5	400.0	0.12
540	402.3	402.3	0.017
545	404.6	404.5	0.031
550	407.1	406.7	0.087
555	409.1	408.9	0.056
560	411.0	411.0	−0.0065
565	413.0	413.2	−0.045
570	415.2	415.3	−0.023
575	417.2	417.4	−0.034
580	419.1	419.5	−0.075
585	421.0	421.5	−0.13
590	423.3	423.6	−0.055
595	424.9	425.6	−0.16
600	426.6	427.6	−0.23
605	429.0	429.6	−0.13
610	431.5	431.6	−0.023
615	433.6	433.5	0.018
620	435.4	435.5	−0.014
625	437.0	437.4	−0.093
630	439.4	439.3	0.0054
635	441.5	441. 3	0.053
640	443.1	443.2	−0.017
645	444.8	445.1	−0.068
650	447.2	447.0	0.053
655	449.1	448.8	0.056
660	450.9	450.7	0.044
665	452.9	452.6	0.066
670	454.6	454.5	0.022

Table 3 Calculated thermodynamic function data of Li_2(2,6-NDC)

T/K	$H_T - H_{298.15}$/kJ mol^{-1}	$S_T - S_{298.15}$/J K^{-1} mol^{-1}
195	−22.68	−92.13
200	−21.78	−87.58
205	−20.86	−83.03
210	−19.92	−78.49
215	−18.96	−73.96
220	−17.97	−69.44
225	−16.97	−64.93
230	−15.94	−60.42
235	−14.90	−55.93
240	−13.83	−51.44
245	−12.75	−46.96
250	−11.64	−42.50
255	−10.52	−38.04
260	−9.372	−33.59
265	−8.207	−29.15
270	−7.023	−24.73
275	−5.819	−20.31
280	−4.597	−15.91
285	−3.355	−11.51
290	−2.095	−7.124
295	−0.8155	−2.750
298.15	0	0
300	0.4823	1.613
305	1.799	5.964
310	3.133	10.30
315	4.486	14.63
320	5.856	18.95
325	7.245	23.26
330	8.651	27.55
335	10.07	31.83
340	11.52	36.10
345	12.97	40.36
350	14.45	44.60
355	15.94	48.83
360	17.45	53.05
365	18.97	57.26
370	20.52	61.46
375	22.07	65.64
380	23.65	69.81
385	25.24	73.96
390	26.84	78.10
395	28.47	82.23
400	30.10	86.35
405	31.75	90.45
410	33.42	94.54
415	35.10	98.62
420	36.80	102.7
425	38.51	106.7
430	40.24	110.8
435	41.98	114.8
440	43.73	118.8
445	45.50	122.8
450	47.28	126.8
455	49.08	130.7
460	50.88	134.7
465	52.71	138.6
470	54.54	142.6
475	56.39	146.5
480	58.25	150.4
485	60.13	154.3
490	62.01	158.1
495	63.91	162.0
500	65.83	165.8
505	67.75	169.7
510	69.69	173.5
515	71.63	177.3
520	73.59	181.1
525	75.57	184.8
530	77.55	188.6
535	79.54	192.3
540	81.55	196.1
545	83.57	199.8
550	85.60	203.5
555	87.63	207.2
560	89.68	210.9
565	91.74	214.5
570	93.81	218.2
575	95.90	221.8
580	97.99	225.4
585	100.1	229.0
590	102.2	232.6
595	104.3	236.2
600	106.5	239.8
605	108.6	243.4
610	110.8	246.9
615	113.0	250.4
620	115.1	253.9
625	117.3	257.4
630	119.5	260.9
635	121.7	264.4
640	123.9	267.9
645	126.1	271.3
650	128.3	274.8
655	130.6	278.2
660	132.8	281.6
665	135.1	285.1
670	137.3	288.4

where $C_{p,m}$(exp) is the experimental molar heat capacities and $C_{p,m}$(fit) is the calculated heat capacities. Based on Eq. 1, the heat capacity of Li_2(2,6-NDC) at 298.15 K was calculated to be 260.0 J mol^{-1} K^{-1}.

Thermodynamic functions

Enthalpy and entropy of substances are basic thermodynamic functions. Through the polynomial representing heat capacity and the relationship between thermodynamic functions and heat capacity, the thermodynamic functions relative to the reference temperature of 298.15 K of this compound were calculated from 195 to 670 K with an interval of 5 K. The thermodynamic relationships are as follows:

$$H_T - H_{298.15} = \int_{298.15}^{T} C_{p,m}dt, \quad (3)$$

$$S_T - S_{298.15} = \int_{298.15}^{T} (C_{p,m}/T)dT. \quad (4)$$

The calculated thermodynamic functions $[H_T - H_{298.15}]$ and $[S_T - S_{298.15}]$ are listed in Table 3. It can be seen that both of the thermodynamic functions $[H_T - H_{298.15}]$ and $[S_T - S_{298.15}]$ of Li_2(2,6-NDC) increase with increasing temperature in a continuous manner in the temperature range from 195 to 670 K.

Conclusions

In this study, a three-dimensional lithium-based metal–organic framework Li_2(2,6-NDC) has been solvothermally synthesized and characterized. The compound has a remarkable high thermal stability up to 863 K under air atmosphere, which is very rare in currently reported coordination polymers. The molar heat capacities of the compound were measured by TMDSC for the first time. The heat capacity of the compound at 298.15 K was calculated to be 260.0 J mol^{-1} K^{-1}. The thermodynamic function data (enthalpy and entropy) relative to the reference temperature (298.15 K) were calculated in the temperature range from 195 to 670 K.

Acknowledgements The authors gratefully acknowledge the financial support for this work from the National Natural Science Foundation of China (No. 2083309, 20873148, 20903095, 50671098, and U0734005), the National Basic Research Program (973 program) of China (2010CB631303), and IUPAC (Project No. 2008-006-3-100).

References

1. Himsl D, Wallacher D, Hartmann M. Improving the hydrogen-adsorption properties of a hydroxy-modified MIL-53(Al) structural analogue by lithium doping. Angew Chem Int Ed. 2009;48:4639–42.
2. Jia C, Yuan XX, Ma ZF. Metal-organic frameworks (MOFs) as hydrogen storage materials. Prog Chem. 2009;21:1954–62.
3. Kusgens P, Rose M, Senkovska I, Frode H, Henschel A, Siegle S, Kaskel S. Characterization of metal-organic frameworks by water adsorption. Microporous Mesoporous Mater. 2009;120:325–30.
4. Uemura K, Maeda A, Maji TK, Kanoo P, Kita H. Syntheses, crystal structures and adsorption properties of ultramicroporous coordination polymers constructed from hexafluorosilicate ions and pyrazine. Eur J Inorg Chem. 2009:2329–37.
5. Wang XS, Ma SQ, Yuan DQ, Yoon JW, Hwang YK, Chang JS, Wang XP, Jorgensen MR, Chen YS, Zhou HC. A large-surface-area boracite-network-topology porous MOF constructed from a conjugated ligand exhibiting a high hydrogen uptake capacity. Inorg Chem. 2009;48:7519–21.
6. Yan Y, Lin X, Yang SH, Blake AJ, Dailly A, Champness NR, Hubberstey P, Schroder M. Exceptionally high H-2 storage by a metal-organic polyhedral framework. Chem Commun. 2009:1025–7.
7. Finsy V, Ma L, Alaerts L, De Vos DE, Baron GV, Denayer JFM. Separation of CO2/CH4 mixtures with the MIL-53(Al) metal-organic framework. Microporous Mesoporous Mater. 2009;120:221–7.
8. Gallo M, Glossman-Mitnik D. Fuel gas storage and separations by metal-organic frameworks: simulated adsorption isotherms for H-2 and CH4 and their equimolar mixture. J Phys Chem C. 2009;113:6634–42.
9. Keskin S, Sholl DS. Assessment of a metal-organic framework membrane for gas separations using atomically detailed calculations: CO2, CH4, N-2, H-2 mixtures in MOF-5. Ind Eng Chem Res. 2009;48:914–22.
10. Liang ZJ, Marshall M, Chaffee AL. CO_2 adsorption-based separation by metal organic framework (Cu-BTC) versus zeolite (13X). Energy Fuels. 2009;23:2785–9.
11. Seo JS, Whang D, Lee H, Jun SI, Oh J, Jeon YJ, Kim K. A homochiral metal-organic porous material for enantioselective separation and catalysis. Nature. 2000;404:982–6.
12. Hong DY, Hwang YK, Serre C, Ferey G, Chang JS. Porous chromium terephthalate MIL-101 with coordinatively unsaturated sites: surface functionalization, encapsulation, sorption and catalysis. Adv Funct Mater. 2009;19:1537–52.
13. Wang MS, Guo SP, Li Y, Cai LZ, Zou JP, Xu G, Zhou WW, Zheng FK, Guo GC. A direct white-light-emitting metal-organic framework with tunable yellow-to-white photoluminescence by variation of excitation light. J Am Chem Soc. 2009;131:13572–3.
14. Wen LL, Wang D, Wang CG, Wang F, Li DF, Deng KJ. A 3D porous zinc MOF constructed from a flexible tripodal ligand: synthesis, structure, and photoluminescence property. J Solid State Chem. 2009;182:574–9.
15. Zhang KL, Pan ZC, Chang Y, Liu WL, Ng SW. Synthesis and characterization of an energetic three-dimensional metal-organic framework with blue photoluminescence. Mater Lett. 2009;63:2136–8.
16. Zhang L, Li ZJ, Lin QP, Zhang J, Yin PX, Qin YY, Cheng JK, Yao YG. Novel (3,6)-connected network and (4,6)-connected framework in two copper(II) and cadmium(II) complexes of flexible (2S,3S,4R,5R)-tetrahydrofurantetracarboxylic acid: synthesis, structure, thermostability, and luminescence studies. Crystengcomm. 2009;11:1934–9.

17. Chen Z, Fei ZF, Zhao DB, Feng YJ, Yu KB. Synthesis, characterization and X-ray crystal structures of lithium coordination polymer from cyclobutane-1,1-dicarboxylic acid. Inorg Chem Commun. 2007;10:77–9.
18. Liu YY, Zhang H, Sun LX, Xu F, You WS, Zhao Y. Solvothermal synthesis and characterization of a lithium coordination polymer possessing a highly stable 3D network structure. Inorg Chem Commun. 2008;11:396–9.
19. Liu YY, Zhang J, Xu F, Sun LX, Zhang T, You WS, Zhao Y, Zeng JL, Cao Z, Yang DW. Lithium-based 3D coordination polymer with hydrophilic structure for sensing of solvent molecules. Cryst Growth Des. 2008;8:3127–9.
20. Banerjee D, Kim SJ, Parise JB. Lithium based metal-organic framework with exceptional stability. Cryst Growth Des. 2009; 9:2500–3.
21. Checoni RF, Francesconi AZ. Measurements of excess molar enthalpy and excess molar heat capacity of (1-heptanol or 1-octanol) + (diethylamine or s-butylamine) mixtures at 298.15 K and 0.1 MPa. J Therm Anal Calorim. 2009;97:747–53.
22. Drebushchak VA. Heat capacity increases with pressure. J Therm Anal Calorim. 2009;95:313–7.
23. Leitner J, Ruzicka K, Sedmidubsky D, Svoboda P. Heat capacity, enthalpy and entropy of calcium niobates. J Therm Anal Calorim. 2009;95:397–402.
24. Lv XC, Tan ZC, Gao XH, Shi Q, Sun LX. Molar heat capacity and thermodynamic properties of crystalline $[Nd(Glu)(H_2O)_5(Im)_3](ClO_4)_6{\cdot}2H_2O$. J Therm Anal Calorim. 2009;95:387–92.
25. Sedmidubsky D, Leitner J, Svoboda P, Sofer Z, Machacek J. Heat capacity and phonon spectra of A N-III. J Therm Anal Calorim. 2009;95:403–7.
26. Yoshida T, Moriya Y, Tojo T, Kawaji H, Atake T, Kuroiwa Y. Heat capacity at constant pressure and thermodynamic properties of phase transitions in PbMO3 (M=Ti, Zr and Hf). J Therm Anal Calorim. 2009;95:675–83.
27. Wunderlich B. The contributions of MDSC to the understanding of the thermodynamics of polymers. J Therm Anal Calorim. 2006;85:179–87.
28. Chau J, Garlicka I, Wolf C, Teh J. Modulated DSC as a tool for polyethylene structure characterization. J Therm Anal Calorim. 2007;90:713–9.
29. Qi YN, Xu F, Ma HJ, Sun LX, Zhang J, Jiang T. Thermal stability and glass transition behavior of PANI/gamma-Al2O3 composites. J Therm Anal Calorim. 2008;91:219–23.
30. Qiu SJ, Chu HL, Zhang J, Qi YN, Sun LX, Xu F. Heat capacities and thermodynamic properties of CoPc and CoTMPP. J Therm Anal Calorim. 2008;91:841–8.
31. Zhang J, Zeng JL, Liu YY, Sun LX, Xu F, You WS, Sawada Y. Thermal decomposition kinetics of the synthetic complex Pb(1, 4-BDC)center dot(DMF)(H2O). J Therm Anal Calorim. 2008;91: 189–93.
32. Archer DG. Thermodynamic properties of synthetic sapphire (Alpha-Al_2O_3), standard reference material 720 and the effect of temperature-scale differences on thermodynamic properties. J Phys Chem Ref Data. 1993;22:1441–53.